9.0 MICROBIAL RESPONSE TO ZINC AND CADMIUM IN PURE CULTURE

From the microcosm study presented in the previous chapter, it was shown although there were changes in the zinc speciation it was difficult to distinguish between the abiotic and biotic effects. This was in large part due to the large number of environmental variables that were difficult to control in such as system. Using a reductionist approach, further study was conducted to examine Lake DePue microorganisms in pure culture. Thus, this reduction in complexity allows better characterization of the interactions between metal-resistant microbes and contaminant metals.

This body of work examines metal-microbe interactions and was composed of several experiments. The first task was to isolate metal resistant bacteria from Lake DePue sediments and microcosms and was undertaken by the Stahl lab. Once microbes were isolated in pure culture, studies were performed focusing on using CS-XAS to analyze the coordination of metals within and on the surface of the cells as well as examining the changes in speciation of the media as a function of substrate utilization. The sections within this chapter will discuss briefly the special techniques used to examine the EXAFS spectra in these experiments, the organisms that were used in this study, and then the differences in the metal coordination and speciation that were observed in each of the microbes.

9.1 Analysis of CS-EXAFS Spectra from Microbial Samples

Pure culture isolates were examined using Continuous Scan Extended X-ray Absorption Fine Structure (CS-EXAFS) spectroscopy to probe the coordination environment of zinc and cadmium associated with the microbial biomass. Cells for these experiments were grown in a minimal nutrient media containing typical salts and nutrients and was buffered at near-neutral pH using the TES buffer. Metal interfering anions, such as phosphate, were reduced as much as possible. Table 9.1 gives the composition of the media.

Table 9.1: Composition of the minimal media used in the CS-XAS studies.

Component	Concentation (mg/L)
NaCl	400
NH_4Cl	400
KCl	0.1
$MgCl_2 * 6H_2O$	330
$CaCl_2 * 2H_2O$	50
$MnSO_4 * H_2O$	5
$CoCl_2 * 6H_2O$	1
$CuCl_2 * 2H_2O$	0.1
$Na_2Mo4 * 2H_2O$	0.1
$NiCl_2 * 6H_2O$	0.1
Riboflavin	0.05
Cyanocobalamin	0.05
Folate	0.02
Thiamine HCl	0.05
Nicotinic Acid	0.05
Lipoic Acid	0.05
TES buffer	2.0

Depending on which organism was being examined, substrates consisted of either crotonate, yeast extract, or glucose. Due to the uncharacterized nature of the yeast extract, its use was minimized as much as possible. The bacteria were allowed to grow in media containing from 500 μM to 5 mM total zinc at circum-neutral pH, and were then separated from the media by filtration through a 0.2μm Nucleopore filter. The filter was then encapsulated in between two strips of Kapton tape, and placed in liquid nitrogen until analysis to preserve the chemical properties of the sample. For extremely dilute samples where filtration was not feasible, the cells were rinsed several times in Milli-Q water to remove excess zinc from the surrounding solution. The biomass was then centrifuged into a thick paste of concentrated cells. This paste was then applied directly to the Kapton tape, sealed, and placed in liquid nitrogen. The spectra were collected and normalized as described in Chapter 4.

To quantify the coordination shells of these samples, two different fitting techniques were employed. Since the biological zinc complex in these bacteria are unlikely to be closely related to a mineral complex, direct comparison to standard model compounds is not likely to result in a clear answer. However, model compounds are very useful in screening the general type of complex detected. Lacking a defined model compound, an *ab initio* calculation can be used to determine the number and type of scatterers around the absorbing atom. However, previous works have shown that some confusion may arise when trying to distinguish Zn-S_4 sites from Zn-S_3O and ZnS_3N sites (Hubbard *et. al.*, 1991; Marmorstein *et. al.*, 1992; Guo *et. al.*, 1995). This is largely due to the fact that in a mixed-shell coordination environment the sulfur and nitrogen scatterers may cause

significant interference with each other, causing a "blurring" of the individual shells (Clark-Baldwin *et. al.*, 1998). Collecting data out to 16 Å-1 can minimize this effect. However, with dilute systems, good quality data to this extent can be very difficult to obtain. Thus, another approach based on the Clark-Baldwin procedure described below, was also utilized.

The Clark-Baldwin fitting procedure successively varied the number of sulfur and oxygen / nitrogen ligands present in a simple two shell fit (Clark-Baldwin *et. al.*, 1998). One advantage of this method is that each fit uses the same number and type of variable parameters. Thus the parameters that characterize the error in the fit, such as the sum of the squared residuals, are directly comparable. *Ab inito* calculations are performed using FEFF8 to calculate the theoretical amplitude and phases of neighboring atoms. Through application of the EXAFS equation (see Section 4.4.1), parameters such as S_0^2 can be found by fitting standard compounds whose coordination shells are well defined. This leaves the major variables in the EXAFS equation to solve for being the number and type of scattering atoms, their distance from the central metal atom, and their associated disorder (Debye-Waller parameter). To reduce the number of variables, the total coordination number of zinc is fixed at four (or six), and the number of oxygen / nitrogen scatterers varied in increments of 0.2. For example, the if the total coordination number is set at four, a series of fits to the EXAFS equation are performed which have defined coordination environments of: 4 sulfur-0 oxygen, 3.8 sulfur-0.2 oxygen, 3.6 sulfur-0.4 oxygen … 0 sulfur-4 oxygen. Fitting was performed on the k^3 weighted EXAFS data. The error of each fit in the series was calculated by:

$$\varepsilon = \sqrt{\sum_{i=1}^{N} \frac{k^6 (\chi_{obs}(k_i) - \chi_{calc}(k_i))^2}{N}}$$

where N is the number of data points in the spectrum. To determine the optimal fit of the series, each fit was compared to a fit of the data by two independent shells of sulfur. This 2S+2S fit is not necessarily physically meaningful, but rather provides a useful measure of the effect of doubling the number of variable parameters (having two types of coordination shells *vs.* a single coordination shell). For example, a 2S+2S fit will nearly always have a lower residual than a fit of four sulfurs in a single shell. Thus, the fractional improvement (P_i) in the *i*th fit can be expressed by:

$$P_i = (\varepsilon_{2S+2S} - \varepsilon_i) / \varepsilon_{4S}$$

where ε_{2S+2S}, ε_{4S}, and ε_i are the error of a fit with two independent 2S shells, the error of a fit with a single 4S shell, and the error of the *i*th fit respectively. The highest P_i for the sample corresponds to the best-fit coordination environment.

However, this technique also has its potential limitations. The original intention for this approach was for use with purified protein systems. In this case, the coordination of a binding site is "well defined" in the manner that it is pure. A coordination environment determined from theory should give a mixture of integral binding sites. In the bacterial systems examined, it is unlikely that there is a single zinc binding site which completely dominates the spectra. The spectra collected can result from a combination of several

different binding sites, both external in internal. Thus, this method was used as a complementary approach to the more traditional FEFFIT simulations (Newville, 2001) described below.

The coordination environment of zinc in these microorganisms was also determined by direct fitting of the EXAFS equation using the FEFFIT routine (Newville, 2001). Again, the routine uses *ab inito* calculated amplitudes and phases for each type of neighboring scatterer as determined by FEFF8. The major difference between the Clark-Baldwin fitting and this fitting procedure is that the total coordination number is not fixed at an integral number and the fitting is performed in a single minimization, rather than through a series of iterations. Parameters in the EXAFS equation such as S_0^2 and e_0 were set as constants as determined from fitting known, standard compounds. The routine then optimizes the fit, obtaining numbers for the number of atoms in each coordination shell, the radial distance of each shell, and the Debye-Waller parameter for each shell. Data were taken over a k-range from 2 to 12 $Å^{-1}$ and then backtransformed over the first coordination shell of the sample. FEFFIT fitting was performed in both backtransformed k-space and in R-space. Minimal differences were observed between the fits of these two data sets. Examples of the scripts used to program the FEFFIT engine are given in the Data Analysis section of Appendix A (Section A.5.3).

9.2 MICROBE ISOLATION AND CHARACTERIZATION

Microbes were isolated into pure culture by Dr. Bradley Jackson in the Stahl lab at Northwestern University. The organisms were obtained from both the microcosm enrichments performed in the previous chapter and from sediments collected directly in the field. Bacteria were isolated into pure culture by using the roll tube method for cultivation of strict anaerobes (Hungate, 1969). Briefly, this method uses an agar medium distributed in a thin layer over the internal surface of a sealed culture tube to support bacterial growth. The inoculum is introduced into the agar before it is rolled into the tube to evenly distribute the microbes within the culture medium. The cultures were kept strictly anaerobic by filling the tubes with an anaerobic, nitrogen atmosphere. Careful anaerobic techniques were used to ensure that no oxygen contamination occurred during the inoculating process (Hungate, 1969). Pure cultures are obtained by a series of sequential dilutions of the individual colonies that develop in the agar.

Morphologies of the isolated organisms range from individual planktonic Gram positive rods to groups of cells that grow in large fibrils up to several hundreds of microns long. All the microbes that were isolated are obligate anaerobes and exhibit tolerance to high zinc concentrations, *i.e.*, show some growth up to a limit of 2 to 5 mM total zinc using yeast extract as a substrate. Isolates also show resistance to cadmium, but at lower concentrations (*e.g.* 500 μM).

A screen of substrate suitability for growth was also performed. Substrates include unsaturated organic acids, amino acids, hydrogen, and simple sugars. Table 9.2 shows a summary of these experiments for two of the studied isolates. Nearly all organisms

Table 9.2: Substrate and acceptor table for two of the DePue isolates as determined by Bradley Jackson. These organisms are selected for display, as they are two of the most thoroughly examined. All electron acceptors were tested with 10 psig hydrogen as the electron donor. Key: + growth; (+) weak growth; - no growth; NT not tested.

Substrate	**Organism X**	**Organism D**
glucose	+	+
fumarate	-	-
pyruvate	(+)	-
citrate	(+)	-
crotonate	-	(+)
casamino acids	(+)	+
yeast extract	+	+
Acceptor		
oxygen	-	-
bicarbonate	+	-
sulfate	-	NT

showed strong growth when yeast extract was used as a substrate or co-substrate. However, the detailed composition of yeast extract is unknown, and makes its use difficult for following metal speciation. This is largely due to the metal binding properties of yeast extract that are significant and cannot be determined easily. Crotonate or glucose was used as common substrates in most of the experiments where minimal metal binding was required.

Preliminary sequence analyses of the highly conserved ribosomal RNA subunits (16S-rRNA) established a phylogenetic relation to members of the low %G+C division within the domain *Bacteria.* A phylogenetic tree for the Lake DePue organisms and their relatives is presented in Figure 9.1. The tree shows that many of the organisms isolated

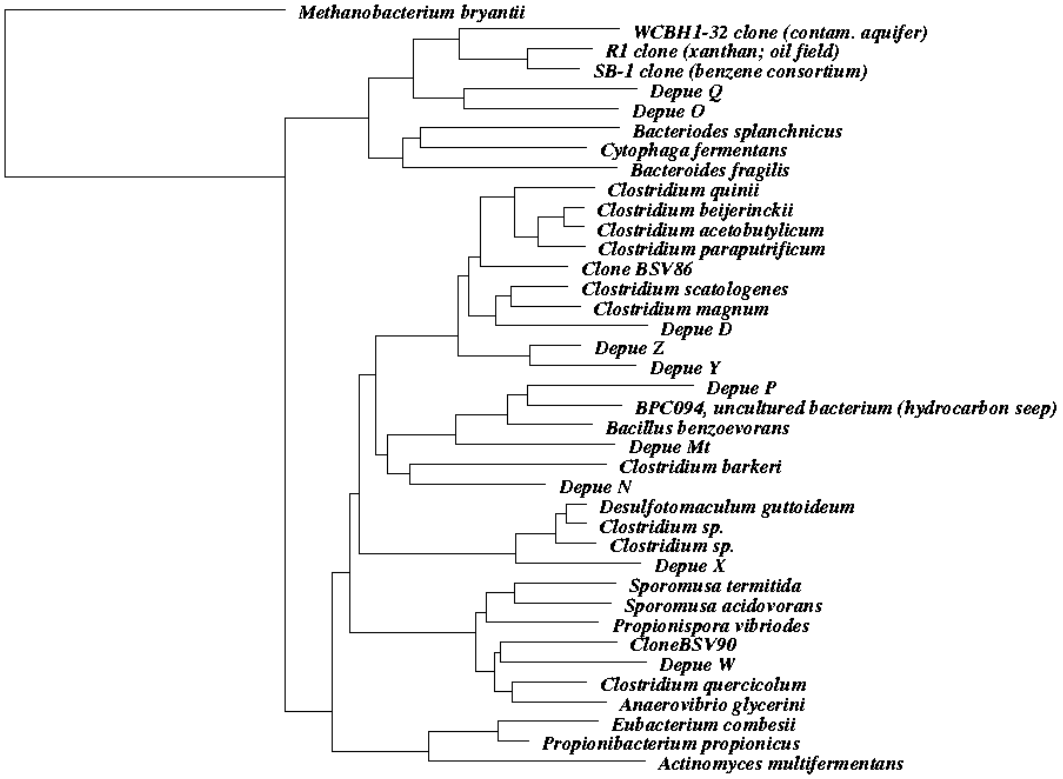

Figure 9.1: Phylogenetic tree of Lake DePue isolates and the nearest related organisms based on sequences of 16S rRNA. Tree was constructed by Bradley Jackson.

are relatively novel organisms, with very few known close relatives based on their 16s ribosomal sequence. In general, the organisms can be classified as belonging to a number of diverse families, including the Clostridia, Bacillus, and Cytophaga groups.

The wide assortment of organisms isolated from these sediments shows that even in very contaminated environments, a remarkable diversity can persist. A common thread that exists in these organisms is that many of the most closely related organisms to the Lake DePue Isolates are clones from other highly contaminated environments.

Before discussing metal coordination of the DePue isolates, a brief summary of each of the major organisms examined in this study is given to familiarize the reader with the class of microbes each one belongs to. Isolates X, Y, Z, and D are all encompassed within the phylotypically and phenotypically diverse clostridia family. Members of this family are ubiquitous throughout the environment. They are capable of a wide range of anaerobic metabolisms, including fermentative, celluloytic, polysaccharolytic, pectinolytic, and acetogenic. The members of the Clostridium genus are generally considered to require anoxic environments for growth (Madigan *et. al.*, 1997). Isolate X shows a sequence that is similar to a highly related group of Clostridia, which differ in their sequence by no more than 5%. The substrates that this group is able to utilize vary widely, although a common metabolism throughout all strains is carbohydrate fermentation. Unlike Isolate X, none of the organisms in the group were isolated from contaminated environments. The closest relatives to organism X are two undescribed bacteria isolated from the rumen of red deer, which hydrolyze lipids and ferment glycerol. Isolate X is also closely related to a bacterium, *Desulfotomaculum guttoideum*, which is able to reduce sulfite or thiosulfite. This has interesting implications for the potential resistance mechanisms of Isolate X, as sulfur compounds generally have a high affinity for zinc and cadmium. Note that while Isolate X is unable to reduce sulfate

(Table 9.2), it has not at this time been tested if it can utilize sulfite or thiosulfite. Organisms Y and Z can grow anaerobically on yeast extract and are most closely related to each other than any of their closest relatives, such as clone BSV86. This organism was obtained from an anoxic rice paddy (Hengstman *et. al.*, 1999) and is probably representative of bacteria that coexist in reduced, methanogenic environments.

Isolate D forms a small phylogenetic cluster with *C. scatologenes* and *C. magnum*. These related *Clostridium* species were isolated from freshwater sediments. Phenotypically, Isolate D shares the ability with *C. scatologenes* and *C. magnum* to form spores and to grow on glucose. All three organisms produce approximately three moles of acetate per one mole of glucose metabolized, suggesting a homoacetogenic mechanism, presumably using the Acetyl-CoA pathway (Madigan *et. al.*, 1997).

Isolate Mt is phenotypically related to several *Bacillus*-like bacteria, although only distantly related through phylogenetic analysis. In this manner, Isolate Mt resembles *B. benzeovorans* in the respect that it grows in long, filamentous structures and that cell propagation occurs within a sheath structure. Although Isolate Mt has been isolated and maintained under fermentative anaerobic conditions, considering the nature of other *Bacillus* species, other types of anaerobic metabolism, such as nitrate, iron, and manganese respiration, might also occur. However, these metabolism have not been tested, and unlike some *Bacillus* species, Isolate Mt cannot live in aerobic environments.

9.3 METAL COORDINATION IN WHOLE MICROBIAL CELLS

The following section will present the results from the CS-XAS analysis of DePue isolates and discuss the implications the observed coordination has for metal speciation within the cells. Qualitatively, the differences in the zinc coordination of the microbes can be seen in the Fourier transforms of the biomass removed from the cultures raised in zinc containing media (Figure 9.2). The EXAFS data on which the Fourier transform was performed are displayed in Figure 9.3. From these representative radial distribution functions (RDFs), a wide variety of coordination environments are observed. The RDF of Organism X suggests that there are primarily scatterers at a pseudo-radial distance of

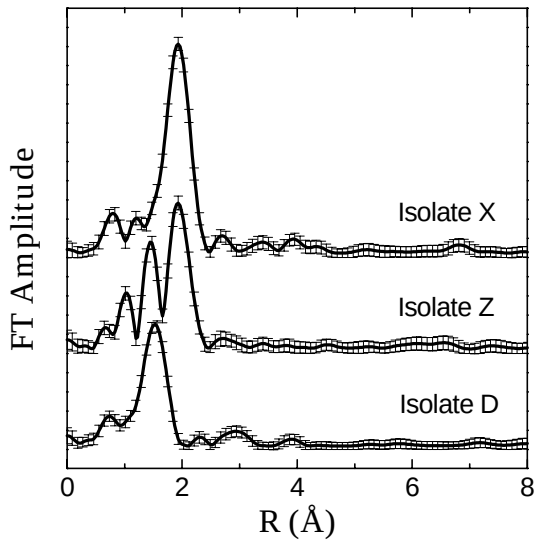

Figure 9.2: Radial distribution functions (RDF) for three of the characteristic isolates examined in the CS-XAS study of microbial cell. Fourier transform taken using the k^3-weighted data from k = 2 to 12 Å. The RDFs are not corrected for phase shifts.

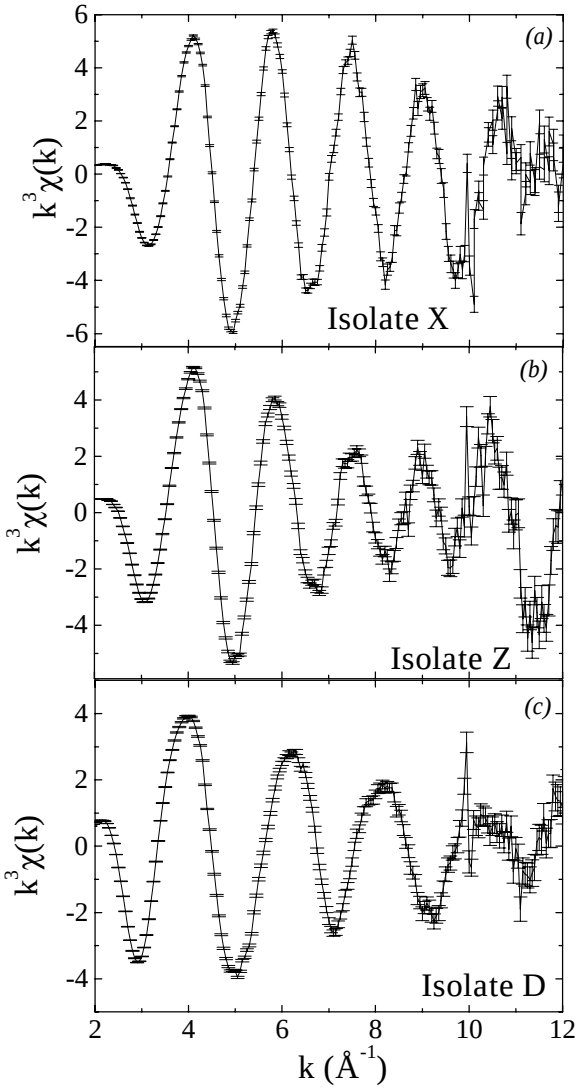

Figure 9.3: EXAFS spectra collected from DePue isolates. Note that the noise level in the data is not significant until large k values.

1.95 Å. Note that this distance is typically a few tenths of an angstrom short, as the RDF has not been corrected for phase shifts. The opposite extreme is Organism D, which has a RDF suggestive of scatterers at 1.5 Å. In contrast to the previous organisms that appear to have a single type of coordination environment, Organism Z shows a combination of ligands, containing scatterers at both 1.95 Å and 1.5 Å. Common ligation

environments for zinc include sulfur, oxygen and nitrogen. Since sulfur has a larger radius than either oxygen or nitrogen, the qualitative nature of these spectra suggest that the coordination varies from sulfur to oxygen / nitrogen, with some species of microbes having mixed coordinations. Since the EXAFS experiment gives an average of all of the zinc coordination environments present in the sample, the results for Organism Z do not necessarily represent an actual mixed shell, *i.e.* a particular zinc atom coordinated to both sulfur and oxygen atoms simultaneously. Rather, another plausible and more likely interpretation of the data is that there is a mixture of zinc binding sites that include both sulfur and oxygen coordination in different physical locations in the cell.

9.3.1 DePue Isolate X

Isolate X showed a strong contribution from sulfur scattering in its EXAFS spectrum. Figure 9.4 shows the results of the modified Clark-Baldwin fitting procedure performed on the EXAFS from the isolates. As described in Section 9.1, the plot is the fractional improvement, P_i, as a function of the percent of sulfur in the coordination shell. The best fit to the data is located at the highest position of the P_i curve. The results show that isolate X is in fact dominated by sulfur coordination, giving an average sulfur coordination of 3.8 and an oxygen / nitrogen coordination number of 0.2. The EXAFS was also analyzed using FEFFIT, shown in Figures 9.5 (a-b). All fitting was performed using the k^3-weighted EXAFS data, using the RDF and the EXAFS spectra as measures of the quality of fit. In Figure 9.5a the real portion of the Fourier transform is displayed along with the magnitude for both the experimental data and the *ab initio* fit to the

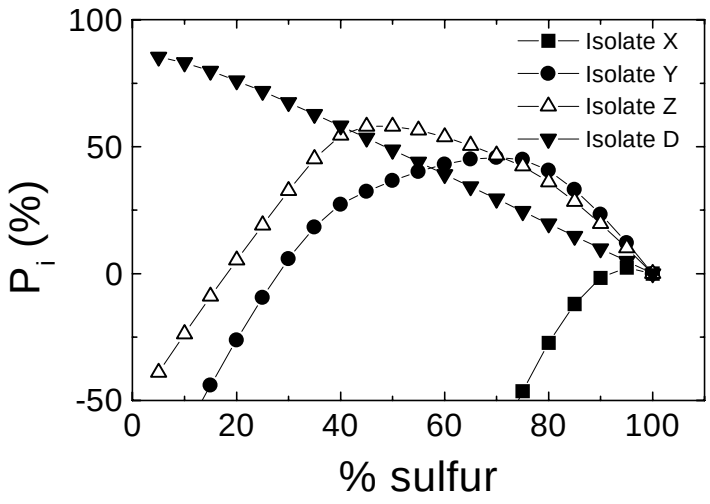

Figure 9.3: Fitting results for DePue organisms using the modified Clark-Baldwin technique. This plot shows the percent improvement of the fit as a function of the sulfur content used in the fit. The best fit is located at the apex of each curve.

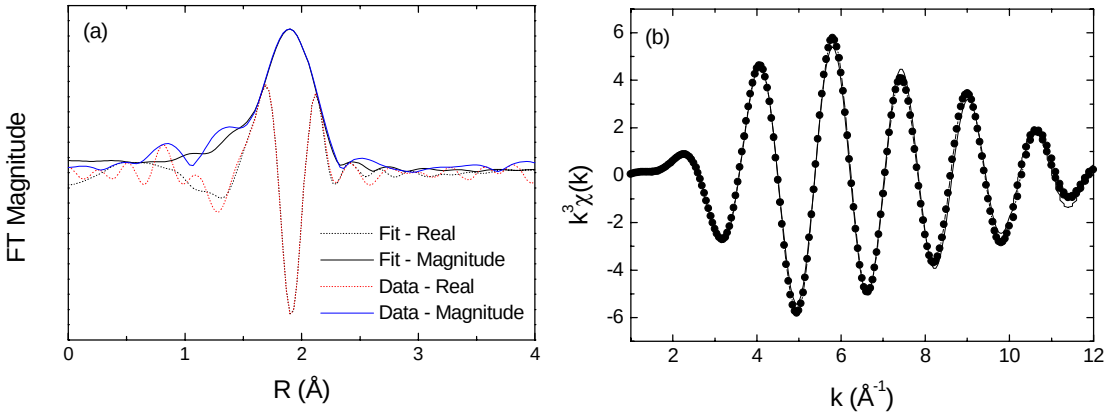

Figure 9.5: FEFFIT fitting results to the EXAFS of Isolate X. **(a)** Fitting results compared to the real portion of the Fourier transform and its magnitude. **(b)** Fitting results compared to the k^3-weighted EXAFS. The data points are the experimental data and the solid line is the fit.

EXAFS. Also shown is the backtransformed EXAFS data of the coordination shell and the fit as determined by FEFFIT in Figure 9.5b. A good fit of the data is observed by the matching phases and amplitude of the EXAFS signal and the fitted data in Figure 9.5b.

This is also verified by examining the real portion of the RDF (Figure 9.5a), which shows that the fit captures the correct phase of the data as well as the magnitude. The results from this fitting give a sulfur coordination number of 3.95 ± 0.5 at an average distance of 2.341 ± 0.021 Å. This distance is characteristic of sulfur coordinated to zinc in thiol configurations as determined by FEFFIT fits to sphalerite (2.320 ± 0.002 Å) and cysteine (2.330 ± 0.003 Å).

The XANES spectra also provide some further details on the type of zinc coordination present in Isolate X. The lack of an intense first peak and early XANES resonances of the microbial four-fold sulfur coordination compared to inorganic ZnS (Figure 9.6) shows

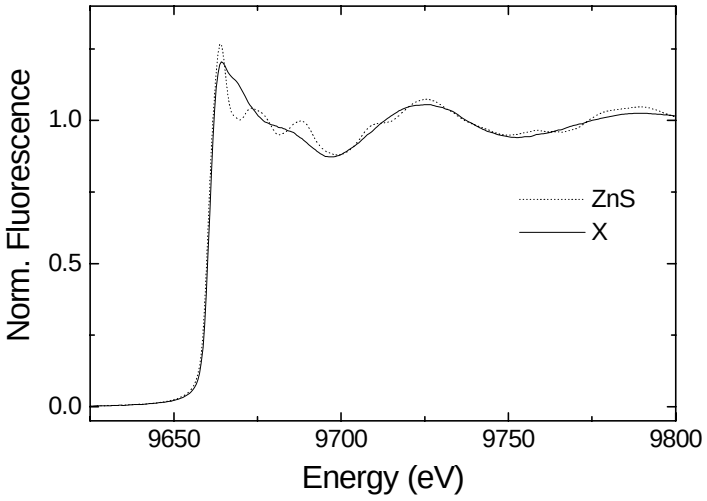

Figure 9.6: XANES features of zinc sulfide (sphalerite) and Isolate X. Note that although the major resonances are the same in both samples, the near-edge resonances present in ZnS are absent from Isolate X. This suggests that although both samples have four-fold thiol coordination, the biological complex is present as a distorted tetrahedral.

that the zinc-sulfur in the isolates is not an inorganic ZnS precipitate. The many resonances that occur in the near-edge spectrum in the inorganic sample are a result of tetrahedral symmetry of the thiol groups. Since Isolate X lacks these strong resonances, the XANES features suggest that the sulfur complex with zinc is an asymetric cellular product. The agreement of these spectra over the slowly varying resonance features supports that Isolate X is coordinated with four thiol groups. Further spectroscopic studies need to be performed in order to characterize any EXAFs features from the second coordination shell of the complex, which did not resolve well in the current study. Low temperature studies of Isolate X may improve the signal, allowing these features to be analyzed.

9.3.2 DePue Isolates D and Mt

These isolates exhibited the same type of coordination with zinc. For the purpose of this discussion, the coordination of Isolate Mt will be examined. These isolates showed the opposite extreme in the qualitative RDF examination in Figure 9.2 appearing to have solely scatterers at oxygen-nitrogen binding distances. The Clark-Baldwin fitting in Figure 9.4 also shows that these isolates completely lack coordination to sulfur. In these cases, the Clark-Baldwin fitting is not the ideal procedure to use, since there is no confusion between mixed coordination shells. Additionally, the constriction that zinc is present in a four-fold coordination state is too limiting, as oxygen is often present in higher coordination numbers.

The FEFFIT fitting results for Isolate Mt are shown in Figure 9.7. The fitting procedure was performed so that coordination numbers higher than four were allowed. Once again, good agreement exists between the collected data spectrum and the *ab initio* fit when viewing the results as both the RDF (Figure 9.7a) and the EXAFS (Figure 9.7b). The fitting was performed using both oxygen and nitrogen parameters. The best fit resulted using oxygen, giving 4.3 ± 0.7 oxygen neighbors at an average distance of 1.933 ± 0.017 Å. Again, this is a typical distance for zinc-oxygen coordination. Distances and coordination numbers of other zinc-oxygen complexes determined by EXAFS are presented in Table 9.3. Fits performed with nitrogen consistently had poorer fitting results than when oxygen was used. However, this cannot rule out the possibility of nitrogen rather than oxygen coordination, as the backscattering amplitudes of the two atoms are very similar. Another possible difficulty with the zinc-nitrogen fitting is that the only standard that was used to calibrate nitrogen scattering was a zinc tetraphenyl

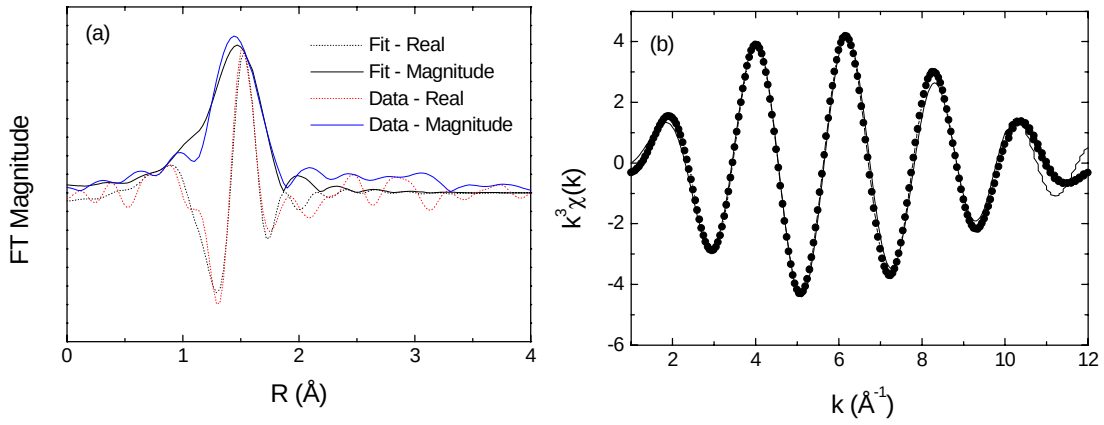

Figure 9.7: FEFFIT fitting results to the EXAFS of Isolate Mt. **(a)** Fitting results compared to the real portion of the Fourier transform and its magnitude. **(b)** Fitting results compared to the k3-weighted EXAFS. The data points are the experimental data and the solid line is the fit.

porphyrin, which may not be typical of the hypothetical zinc-nitrogen binding sites in the microbes.

Table 9.3: Coordination numbers (CN) and bond distances of typical zinc-oxygen compounds. The error on the coordination number of aqueous zinc is zero since it was used as the calibration standard. Zinc complexes of organic acids were performed in aqueous solution with a 200 fold concentration excess of ligand over metal at a pH of 6.5.

Compound	**CN**	**Distance (Å)**
Aqueous Zn	6.0 ± 0.0	2.347 ± 0.002
Smithsonite ($ZnCO_3$)	4.8 ± 0.2	2.329 ± 0.003
Zinc Glutamate	5.0± 0.6	2.072 ± 0.011
Zinc Citrate	5.6 ± 0.4	2.076 ± 0.007
Zinc Salicylate	6.2 ± 0.4	2.081 ± 0.007
Zinc Oxalate	6.3 ± 0.6	2.087 ± 0.011
Zinc Phosphate	3.9 ± 0.1	1.958 ± 0.003

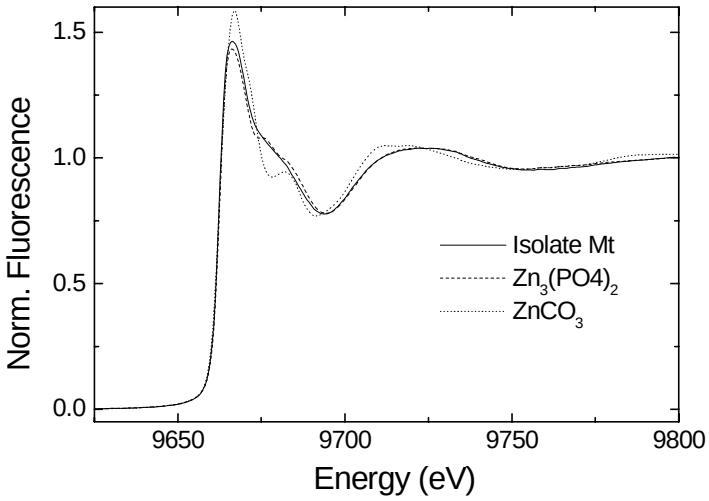

Figure 9.8: XANES spectra of Isolate Mt and oxygen containing zinc compounds. XANES features suggest that phosphoric ligand groups may dominate the zinc binding in the isolate.

The XANES spectra for oxygen coordination can be useful in conjunction with the EXAFS results. The isolates dominated by oxygen / nitrogen coordination show XANES features (Figure 9.8) that are nearly identical to zinc-phosphate. The XANES features of zinc-carbonate are also given to show that similar oxygen coordinated species have significantly different XANES resonances. This suggests that phosphoryl groups may dominate the zinc ligation in these microbes. This is supported by similar EXAFS work examining zinc speciation on the surface of the fungus *Penicillium chrysogenum* cell wall, which shows that surface binding is dominated by phosphoryl groups (Sarret *et. al.*, 1998).

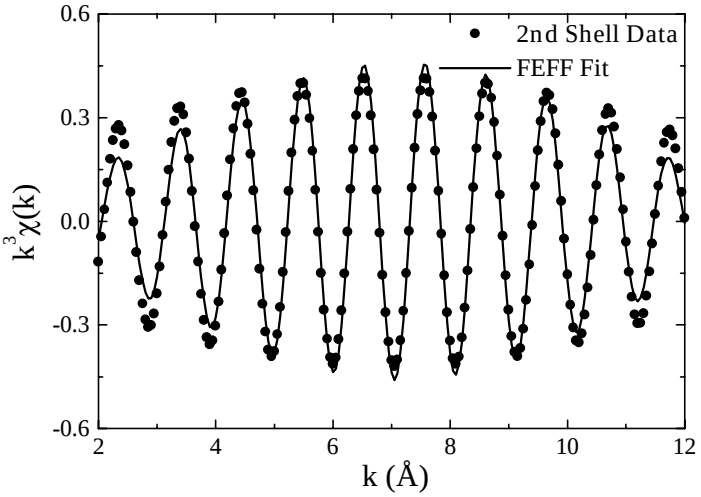

Figure 9.9: FEFFIT fit of the second coordination shell of Isolate Mt with phosphorus neighbors.

Although there is not a strong second shell for phosphorus present in the EXAFS, there is a small peak in the RDF that is significant over the errors (Figure 9.2). Again, we can fit this shell with ab initio calculations using FEFFIT. As shown in Figure 9.9, a good fit result using phosphorus neighbors for the second coordination shell. If carbon is used as the backscatterer in this shell, then as a result, negative numbers of neighbors are present in the second shell. This is due to phosphorus and carbon having opposite phase shifts in the EXAFS equation. The fit results in the second shell of Isolate Mt consisting of 2.8 ± 1.0 phosphorus neighbors at a distance of 3.39 ± 0.09 Å. The larger uncertainties than FEFFIT results from the first coordination shell are due to the fact that the second shell is of smaller amplitude and subject to more disorder and thus more noise. Further evidence of the phosphoric binding in Isolate Mt can bee seen in the examination of the imaginary part of the Fourier transforms. This shows that this

second shell present in Isolate Mt coincides with the phosphorus shell in zinc-phosphate (Figure 9.10) and is out of phase with the Zn-C shell of zinc-carbonate.

The phosphoryl binding in isolate Mt is most likely Zn bound to the outside of cell

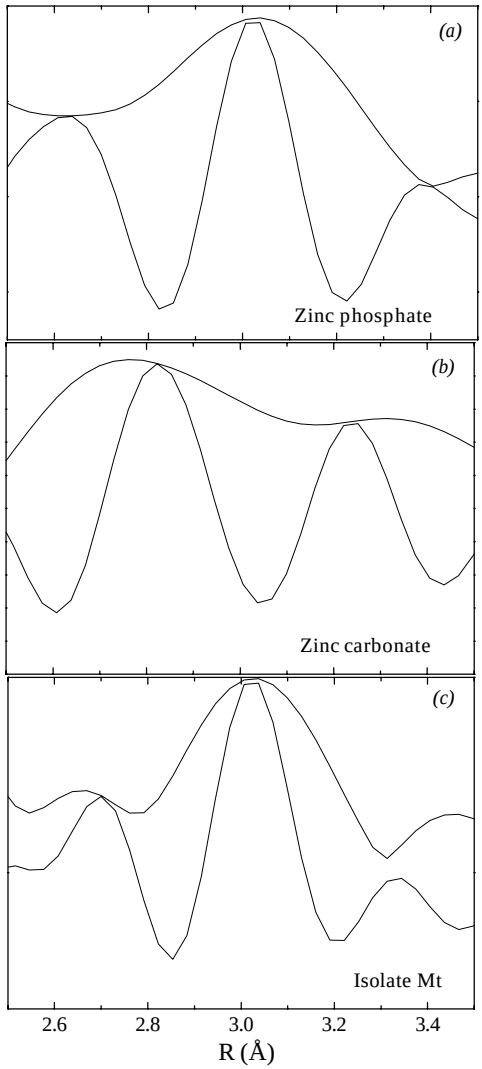

Figure 9.10: Fourier transforms of the second coordination shells of: **(a)** zinc phosphate, **(b)** zinc carbonate, and **(c)** Isolate Mt. Note that the positions and phases of the second shell of Isolate Mt agree best with phosphate.

structures such as the cell membrane. Zinc has been shown in the literature to have a high affinity for binding to phosphoryl sites (Sarret *et. al.*, 1988). The process of zinc absorption onto cell walls should occur for all isolates. However, the zinc examined in these microbes is likely to be a combination of internal and external zinc since the cells were exposed to zinc media throughout the logarithmic growth phase. The strength of the XAS signal from the samples was too large to result from just surface bound species. This was also true for the samples involving DePue Isolate X, which displayed sulfur coordination. This suggests that these isolates that have dominantly sulfur in their coordination environment have an internalization process that sequesters zinc into sulfide or thiol type ligands whose signal swamps out the signal of the surface phosphoryl binding.

9.3.3 DePue Isolate Z

Isolate Z exhibits a coordination environment that is intermediary between that of Isolate X and Isolate Mt. The RDF in Figure 9.2 showed that there were two peaks in the first coordination shell, suggesting that zinc is bound to both sulfur and oxygen / nitrogen. Clark-Baldwin fitting of the data gives a coordination that is approximately 50% sulfur and 50% oxygen. Applying FEFFIT gives similar results with 2.5 ± 0.6 sulfur neighbors and 1.6 ± 0.5 oxygen neighbors at distances of 2.311 ± 0.021 Å and 1.955 ± 0.038 Å respectively. Figure 9.11 shows the resultant fits. Once again, it is important to remember that the EXAFS is sensitive to the average coordinative environment within the cell. The mixed shell that Isolate Z appears to have could

consist of either a protein that has both oxygen and sulfur binding sites, or it could

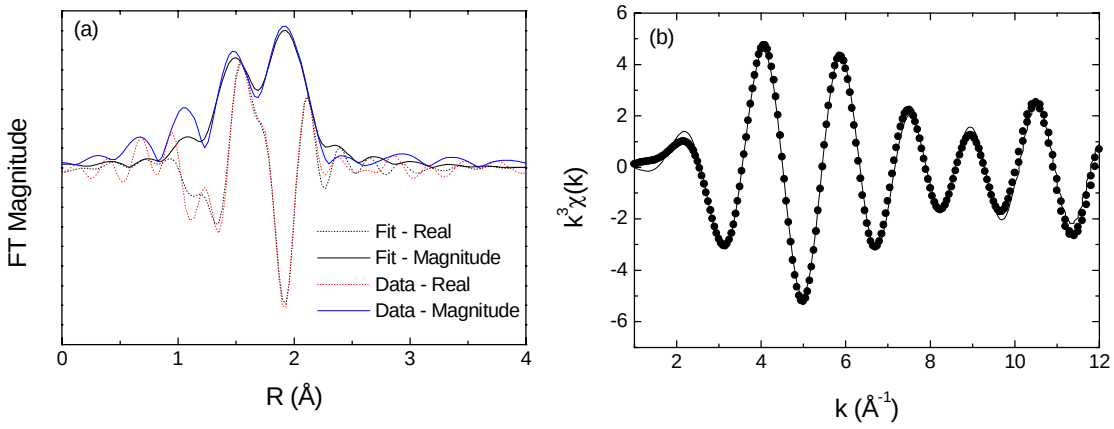

Figure 9.11: FEFFIT fitting results to the EXAFS of Isolate Z. **(a)** Fitting results compared to the real portion of the Fourier transform and its magnitude. **(b)** Fitting results compared to the k3-weighted EXAFS. The data points are the experimental data and the solid line is the fit.

represent a mixture of two types of unique binding sites. One of these could be similar to that of Isolate X, and the other representative of phosphoryl binding as in Isolate Mt.

9.3.4 Cadmium Binding in DePue Isolate X

The binding environment of cadmium with the Isolate X was also looked at briefly. The experiment was performed in an analogous manner as the zinc experiments, with the exception that the metal exposure was 500 μM total cadmium. Even with a reduced quantity of metal added to the media, the isolates showed much slower growth, suggesting that the toxicity of the microbes to cadmium is greater than that of zinc.

Initially, it was thought that since cadmium and zinc are similar in their chemistry (*i.e.*, same column in the periodic table) they might share similar metal binding sites in the cells. However, these experiments showed a stark difference in the way that these metals are coordinated. Unfortunately, the XANES region of the cadmium spectra is extremely similar for nearly all oxygen coordination environments. This eliminated the possibility of the XANES data to help distinguish the cadmium-oxygen coordination of the isolates.

Figure 9.12 shows a sample spectrum from Isolate X and its associated radial distribution function. As noted above, Isolate X coordinates zinc almost exclusively a sulfur environment. However, as can be seen in the case of cadmium, the first shell bond lengths are significantly shorter than cadmium-sulfide bonds, suggesting coordination with either oxygen or nitrogen. Theoretical fitting with *ab initio* parameters

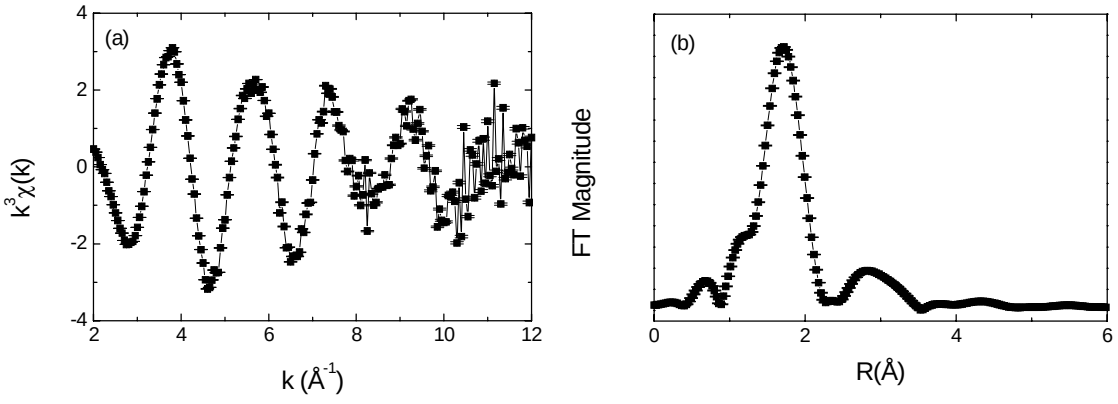

Figure 9.12: Cadmium K-edge EXAFS data of Isolate X. **(a)** k3-weighted EXAFS with associated error bars. **(b)** Fourier transform, uncorrected for phase shift.

from FEFF8 was performed on the spectra to determine the most likely coordination of the cadmium in the isolates. The EXAFS fitting results from these experiments along with several cadmium standards are presented in Table 9.4. The results suggest that an oxygen-like environment dominates the coordination of cadmium in the microbes. However, the average cadmium-oxygen bond distance is intermediate to that of the typical cadmium-oxygen bond and cadmium-nitrogen bond.

Table 9.4: First shell coordination numbers (CN) and bond lengths as determined from CS-EXAFS data fitted by *ab initio* parameter from FEFF8. An error of zero on the CN of some samples denotes that it was used as a standard for calibration purposes. TPP = tetraphenyl porphine.

Compound	CN	Distance (Å)
Cadmium Sulfide	4 ± 0	2.528 ± 0.003
Cadmium-Cysteine	3.9 ± 0.1	2.499 ± 0.002
Aqueous Cadmium	6± 0	2.251 ± 0.003
Cadmium TPP	4 ± 0	2.158 ± 0.002
Cadmium Phosphate	5.6 ± 0.1	2.264 ± 0.002
Cadmium Carbonate	4.8 ± 0.4	2.246 ± 0.007
Cadmium Citrate	5.8 ± 0.4	2.270 ± 0.006
Cadmium Salicyclate	6.1 ± 0.2	2.239 ± 0.002
Isolate X (oxygen)	5.0 ± 0.2	2.217 ± 0.006

The second shell analysis strongly suggests the presence of phosphorus, although again at shorter than the typical inorganic hydrated cadmium phosphate compounds. The FEFFIT fitting gives a coordination number of 1.9 ± 0.1 phosphorus atoms at a distance of 3.34 ± 0.02 Å. It is unlikely that the cadmium on the microbes is in the same form as

the crystalline $Cd_3(PO_4)_2$ standard. The crystalline cadmium phosphate complex itself is a complex compound, with cadmium existing in 5-fold oxygen coordination 45% of the time, and 6-fold oxygen coordination 55% of the time. This leads to the average coordination number of 5.6 for cadmium in cadmium phosphate and an average of 4 phosphate groups surrounding each cadmium center. Since the coordination number of cadmium to oxygen and phosphorus in the samples is consistently smaller in the microbe samples than that of the inorganic complex, the cadmium is likely to exist in a less compact and less ordered environment.

By examining the resolved coordination numbers and bond distances, a picture of the cadmium adsorption environment can be developed. The complex cannot be a monodentate, mononuclear complex, since the preferred geometry in this case would be close to linear. This would lead to a cadmium-phosphate separation of nearly 3.7 Å.

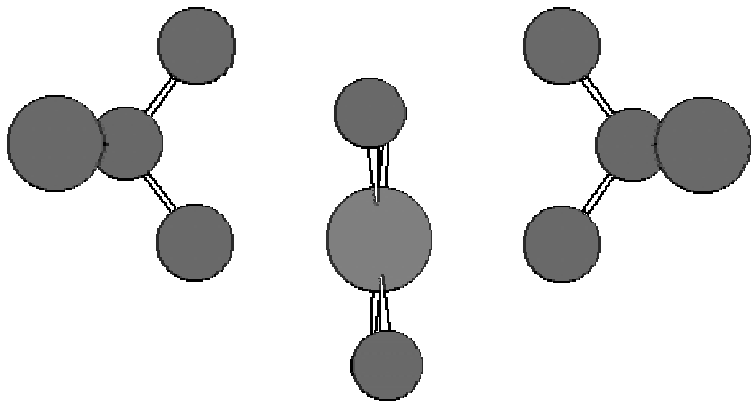

Figure 9.13: Model for the proposed geometry of cadmium bound in microbial biomass. Cadmium is denoted as the grey atom, oxygen by red atoms, and phosphorus by the purple atoms.

Similarly, the complex will not be a bidentate, mononuclear complex either, since this geometry leads to a phosphate distance of 2.75 Å. Thus the complex is at an intermediate distance, suggesting that it would be bidentate, binuclear complex. This is further supported by the fact that the average coordination number of phosphorus around cadmium is two. Thus, there are approximately two phosphate groups that surround each cadmium center. This is half of the value of phosphates that occurs in crystalline $Cd_3(PO_4)_2$. In the simplest analogy, the cadmium complex on these surfaces can be pictured as half of the coordination environment of the solid, with the "outside" of the cadmium coordinated by solvent water. FEFF8.10 was used to construct the *ab initio* EXAFS spectrum of a hypothetical model in which cadmium was complexed to two phosphate tetrahedrals. The proposed geometry is shown in Figure 9.13. The model results and experimental data are shown in Figure 9.14. It can be seen that this model fits the data reasonable well. Most of the features and amplitudes are observed, as well as matching the phases. It is also important to note that the fitting of the data using both the first and second shells simultaneously provided a better fir than the attempts to fit the shells individually. This provides a plausible, although not necessarily unique, structure of cadmium bound within the cell. There are likely several different geometries that exist that could satisfy the observed bond distances and coordination orders. However, the important conclusion is that the cadmium appears to be bound in a binuclear, bidenate fashion to external phosphoryl groups. These proposed groups are most likely to be located at the cell surface. This conclusion is due to the fact that the cadmium is bound with what appears to be a "free" boundary on one side, *i.e.*, the microbial sample has half the number of phosphorus atoms coordinated in

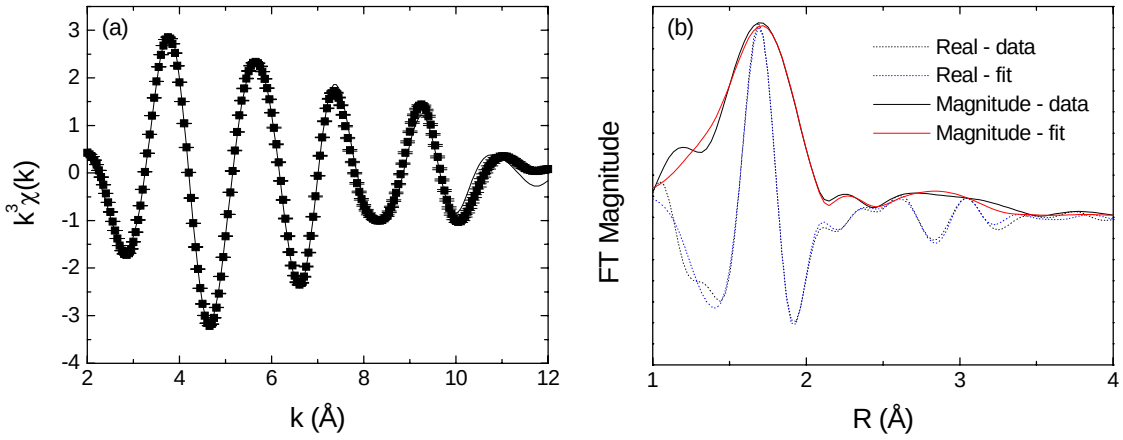

Figure 9.14: Results of applying *ab initio* parameters from FEFF8 based on the model geometry given in Figure 9.13. **(a)** Fit to the backtransformed EXAFS signal. Forward transform over 2-12 $Å^{-1}$, backtransform from 0.9-3.75 Å. **(b)** Fit displayed in R-space, showing the magnitude and real portion of the transform.

the second shell as the phosphate solid. This free boundary suggests that the cadmium is not bound within a larger lattice structure and is most likely a surface-bound type structure. Since phosphoryl groups will have their greatest densities in cell walls, the reasoning above leads to cadmium binding in this organism taking place at the cell surfaces.

9.3.5 Coordination of Zinc to Bacterial Cell Walls

EXAFS studies were carried out to examine the pH dependence of zinc binding to the cell walls. In these experiments, cells of DePue Isolate Z were raised on crotonate as a substrate in the absence of zinc. The cells were collected, gently centrifuged, rinsed and washed in Milli-Q water. The process of centrifigation and washing was repeated with a

solution of 0.01 M EDTA and water again to cleanse excess metals from the cell walls. The dilute solution of EDTA was used in order to insure that the EDTA would not destroy the integrity of the cell walls. The cells were observed to be intact microscopically after this step was completed. The cells were then suspended in solutions of 0.1 M NaCl and 2 mM $ZnCl_2$. The pH of the solutions was adjusted with either NaOH or HCl to the desired pH, between 4 and 8. Cell suspensions were exposed to the solutions for approximately 2 hours. The length was chosen so that adsorption processes had enough time to saturate the cell surfaces, yet uptake into the organism would be minimized. Similar experiments using uranium binding to the cell walls of *B. subtilis* have shown that adsorption equilibrium occurs within approximately 30 minutes and is stable through at least 24 hours (Fowle *et. al.*, 2000). The composition of binding was calculated using the spectral deconvolution method described in the Methods (Chapter 4). The basis set for the analysis consisted of three main coordination types: sulfide, carboxyl, and phosphoric. In addition to monitoring the EXAFS signal, the raw step height of each sample was measured. When normalized to account for amplifier gains, the step height is directly proportional to the amount of zinc that is present in the sample. Since each sample was prepared carefully in order to minimize the differences in sample quantities, this observation provides a measurement of the amount of zinc that was absorbed on the cells. It is important to note that this technique gives the relative concentration difference between samples, as no formal calibration was performed to quantify zinc concentrations as a function of edge height.

Results of the pH experiments are shown in Figures 9.15 and 9.16. As might be expected, distinct trends in both the quantity and quality of absorption can be seen. First, in Figure 9.15, a typical absorption step can is observed, *i.e.* the net absorption edge height is seen to rise as a function of pH as the protons no longer compete with the metal for ligand binding sites on the cell surface. The step is observed to occur just above pH 5. In Figure 9.16, the average coordination environment of zinc on the cell wall is displayed. In all cases, there appears to be small amount of zinc-sulfur coordination. This is most likely due to the fact that some internalization, although small, will occur during the exposure time. Isolate Z was shown in the cell EXAFS studies to have a significant portion of its zinc present in zinc-sulfur coordination. Thus, if internalization did occur, some portion of that would be expected to be in a zinc-sulfur form. However, since the X-ray absorption step height signal of the samples was at least 20 times less

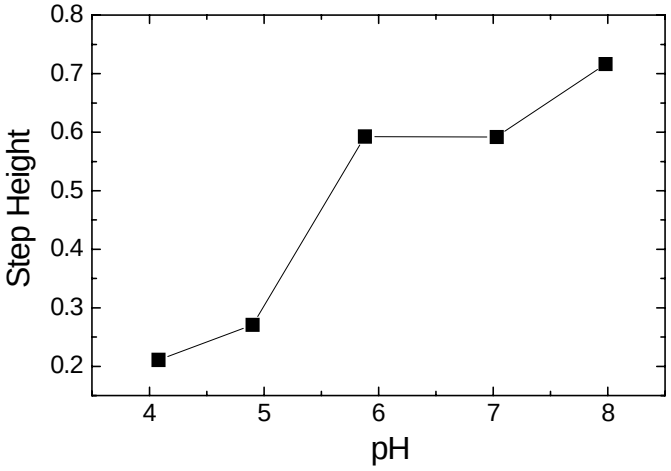

Figure 9.15: Relative height of the K absorption edge of zinc as a function of pH in DePue Isolate Z. Note the strong increase in absorbed zinc for pH values greater than 5. Cells were exposed to Zn_{tot} = 2 mM, I = 0.1 M.

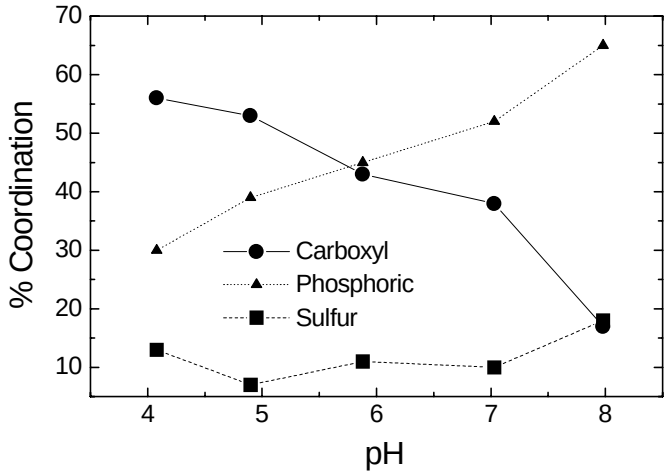

Figure 9.16: Coordination at the cell wall of Isolate Z as a function of solution pH as determined by EXAFS spectral deconvolution. Cells were exposed to Zn_{tot} = 2 mM, I = 0.1 M.

than that of the whole cell internalization experiments described in Sections 9.3.1 through 9.3.3, it was concluded that the greater portion of the zinc measured in this experiment was mostly bound on cell surfaces. If significant internalization had occurred, the step height of the X-ray absorption edge would expected to be much larger than observed in these samples.

The bulk of the zinc coordination environment consisted of either phosphoric or carboxyl ligands. This is not surprising, as these are two of the major types of functional groups found on cell wall structures (Madigan *et. al.*, 1997). These functional groups arise from teichoic acid residues in the peptidoglycan of the Gram positive cell wall. Teichoic acids include all wall, membrane, and capsular polymers that contain glycerophosphate residues. They are bonded covalently by phosphate esters to the peptidoglycan and often have sugars attached as well (Madigan *et. al.*, 1997). Also

found in the peptidoglycan of Gram positive bacteria are teichuronic acids, which are composed of linear polysaccharides with uronic residues (Cox *et. al.*, 1999). Thus, teichoic acids and teichuronic acids can provide phophoryl and carbonyl binding sites respectively in the cell wall.

As the pH was varied, the dominant oxygen coordination shifted from carboxyl at low pH, to phosphoric at high pH. This result matches what is expected from typical acidity constants of these binding groups on cell surfaces measured by other investigators (Fein *et. al.*, 1997; Cox *et. al.*, 1999). The study by Cox, *et. al.*, 1999, gives proton binding constants (apparent pK_a) for these groups as approximately 5.25 for carboxyl type sites and 6.7 for phosphoric type sites. Thus as the pH shifts from low to more neutral values, one expects the see the observed shift in preferred binding sites. Additionally, the amount of zinc that is absorbed to the cell wall as determined by the height of the X-ray absorption edge (Figure 9.15) also increases as the pH increases above each of these proton-binding constants. This supports the premise that zinc will displace the proton, as these sites have a weaker affinity for the proton at higher pH.

9.4 SUMMARY

Overall, the most striking result from these experiments was the discovery of such a wide range of zinc coordination environments among the isolates from Lake DePue. All of the organisms were isolated in under very similar conditions of zinc exposure, yet

many of them displace vastly different coordination properties. Table 9.5 summarizes the fitting results of the CS-XAS data collected for the DePue isolates. These results show that many of the microbes isolated from the DePue system actively changed the speciation of zinc added to the media. These changes are those of internalizing zinc into the organism and coordinating the zinc with various ligands. Of particular interest are Isolates X, Y, and Z that coordinate zinc into a thiol complex. The XAS also shows that the thiol complex found in these organisms is not an inorganic zinc sulfide. Thus, the zinc incorporated into these cells must be tied up into some type of protein or other organic thiol-containing ligand. In addition, Isolate X appeared to amass a substantial amount of zinc within the cell. This was observed by the fact that the XAS samples for

Table 9.5: Summary of fitted values for Lake DePue Isolates. The degree of disorder (DeBye-Waller factor), σ^2, and the goodness of fit (R-value) are also given. The R-value estimates what fraction of the data points are "misfits". Thus for the values in the table below, approximately 1% of the data points are not fit within the error of the fit.

Organism	Me-L	CN	Dist. (Å)	σ^2	R-value
Isolate X	Zn-S	3.95 ± 0.5	2.341 ± 0.021	0.007 ± 0.001	0.0098
	Cd-O	5.0 ± 0.2	2.217 ± 0.006	0.009 ± 0.001	0.0150
	Cd-P	1.9 ± 0.1	3.34 ± 0.02	0.008 ± 0.005	
Isolate Mt	Zn-O	4.3 ± 0.7	1.933 ± 0.017	0.006 ± 0.001	0.0111
	Zn-P	2.8 ± 1.0	3.39 ± 0.09	0.009 ± 0.004	0.0160
Isolate Z	Zn-S	2.5 ± 0.6	2.311 ± 0.021	0.005 ± 0.002	0.0122
	Zn-O	1.6 ± 0.5	1.955 ± 0.035	0.001 ± 0.002	
Isolate Y	Zn-S	3.1 ± 0.6	2.341 ± 0.014	0.007 ± 0.002	0.0095
	Zn-O	1.1 ± 0.5	1.972 ± 0.018	0.001 ± 0.002	

the isolate consistently had a large signal, compared to the other isolates. Not only does Isolate X tie up zinc into a new coordination, but it also appears to internalize it rather than export the metal outside of the cell membrane. Further work may focus on isolating and characterizing the complex in a purer form than in the microbial biomass. Isolate X is also intriguing in the fact that cadmium has a completely different behavior when exposed to the cells. This is surprising, since cadmium and zinc are very similar in their chemical properties and both display similar high binding affinities for sulfur containing ligands. The cadmium results suggest that instead the metal being bound in a thiol protein complex like zinc, the metal is bound into a phosphate complex. Although previous works have shown that intercellular cadmium phosphate granules can form in bacteria such as *Acinetobacter johnsonii* (Boswell *et. al.*, 1999), the EXAFS coordination numbers of phosphate in the second shell infer a surface complex of cadmium and phosphate rather than cadmium in a mineralized matrix.

The phosphate complexation of both cadmium by Isolate X and zinc by Isolates Mt and D is another interesting result of these experiments. As observed in Chapters 6 and 7 by both AEM and XAS, a significant portion of zinc in the sediments of Lake DePue is in the form of phosphate complexes. This could further point to the biological influence of the speciation of zinc in the lake. If the isolates can be shown to form globules of iron and zinc phosphates under similar conditions in the sediments, it would point to a significant control of the zinc speciation on a macroscopic scale. This would also have to be verified by showing that these isolates are truly representative of the natural

populations in the sediment, rather than just the organisms that can be easily cultured in the lab.